PREPARATION AND CHARACTERIZATION OF POLYHYDROXYBUTYRATE/POLYCAPROLACTONE/Mg-Al LAYERED DOUBLE HYDROXIDE NANOCOMPOSITES

CHA PING LIAU[a], MANSOR BIN AHMAD[a,]*, KAMYAR SHAMELI[a b], WAN MD ZIN WAN YUNUS[c], NOR AZOWA IBRAHIM[a], NORHAZLIN ZAINUDDIN[a], YOON YEE THEN[a]

[a]Department of Chemistry, Faculty of Science, Universiti Putra Malaysia, 43400 UPM Serdang, Selangor, Malaysia
[b]Nanotechnology and Advance Materials Department, Materials & Energy Research Center, Karaj, 31787/316, Alborz, Karaj, Iran
[c]Faculty of Defence Science and Technology, National Defence University of Malaysia, Sungai Besi Camp, 57000 Kuala Lumpur, Malaysia

Anionic clay Mg-Al Layered double hydroxide (Mg-Al LDHs) of Mg/Al-NO$_3^-$ with M^{2+}:M^{3+} (3:1) ratio was synthesized by co-precipitation method from nitrate salt solutions were used with continuous agitation at constant pH 9. Beside, modification of nitrate anions by stearate anions between the LDH layers had carried out through ion exchange reaction. Polyhydroxybutyrate (PHB)/Polycaprolactone (PCL)/stearate Mg-Al Layered Double Hydroxide (LDH) nanocomposites were prepared via solution casting intercalation method. FT-IR spectra showed the presence of carboxylic acid (COOH) group indicates that stearate anions were successfully replacing the nitrate anions in the interlayer Mg-Al LDH. The XRD results showed that increasing basal spacing from 8.66 to 32.97 Å in modified stearate Mg-Al LDH. Additional of 1.0 wt % stearate Mg-Al LDH resulting higher basal spacing where polymer chain intercalated into interlayer LDH and TEM results revealed that the 1.0 wt % stearate Mg-Al LDH layers are homogeneously distributed in the PHB/PCL polymer blends matrix. TGA characterization proven that 80PHB/20PCL/1stearate Mg-Al LDH has lower weight loss and higher thermal stability. Enhancement in 300% elongation at break and 66% tensile strength in the presence of 1.0 wt % of the stearate Mg-Al LDH as compare with PHB/PCL blends. Scanning electron microscopy (SEM) proved that clay improves compatibility between polymer matrix and the best ratio 80PHB/20PCL/1stearate Mg-Al LDH surface was well dispersed and stretched before it breaks.

1. Introduction

In the last decades, the production and the use of plastics which synthetically derived from petroleum with not readily biodegradable have been gradually increased. Meanwhile, the amounts of plastic waste disposal have increased particularly in packaging application. Plastic waste consists of high degree of contamination which requires high energy cost to recycle [1]. The development of biodegradable polymers has attracted a great deal of interest recently. Most of the biodegradable polymers are mainly polyester. These polyesters are promising materials for the production of high performance and environment friendly biodegradable plastics. The biodegradable polyesters including polyhydroxybutyrate (PHB), polycaprolactone (PCL),

*Corresponding authors: mansorahmad@gmail.com

poly(lactic acid) (PLA) and poly(butylenesuccinate) (PBS). Although biodegradable polyesters have started making inroads into the commercial application, they are far from becoming substitutes for traditional non-degradable polymers. The major reason is the disadvantageous properties of these materials, such as poor mechanical properties and poor processibility, which limit their application. Taking this situation into consideration, we can understand the necessity and urgency of modification to these polymers.

Polyhydroxybutyrate (PHB) is natural thermoplastic polyester which produced by bacterial fermentation [2] with high biodegradability and biocompatibility. Some of the drawback such as brittleness, inherent rigidity, high production cost and low melt stability limit its applications. In order to overcome the drawbacks of PHB, blending with flexible, biodegradable and high mechanical properties polycaprolactone (PCL) which is an synthetic thermoplastic polyester produced from ring opening polymerization of ε-caprolactone [3] and chemical synthesis of crude oil. The purpose of blending is to achieve intermediate or even superior properties while preserving the major characteristics of the pure components [4]. Much of the attention on polymer/clay nanocomposites have been made to improve the flexibility, compatibility and mechanical properties of polymer blends with additional of small filler concentration. The properties of nanocomposites depend on the dispersion of filler content and adhesive interaction between polymer matrix and filler [5-21].

Layered Double Hydroxides (LDHs) are anionic clays with the structure where positively charged metal hydroxides layer with anions located at interstitial position. Additionally, it's an advanced additive with the advantages high capacity anion intercalation, environmental friendly, economic, naturally abundant [22, 23], nontoxic materials, and room temperature preparation [24]. Hydrophilic character of LDHs restricts the polymer chain intercalated into interlayer of LDHs. Therefore, chemical modification involving was incorporating with long chain organic surfactant anion intercalation to reduce its hydrophilicity [25, 26]. The aim of modification is to enlarge the interlayer distance and make LDH more hydrophobic [27].The unusual packing of the organic anions in LDH gallery may facilitate their easier incorporation into polymers, leading to better nanocomposites formation [28].

Costa et al. [29] was reported with the preparation of intercalation of Mg-Al LDH by anionic surfactants reveal increment in interlayer distance of modified Mg-Al LDH depending on the length of the surfactant anions. Furthermore, Sanchez-Garcia et al. [30] was carried out solution cast composites preparation due to the melt instability of PHB will direct melt compounding. Besides, they were proved that addition of PCL component lead to a finer dispersion of the clay with intercalated morphologies and exhibited improved thermal stability. Sang-Rock et al. [31] proved that the strong hydrogen bonding interaction between biodegradable aliphatic polyester and organo-clay will lead to higher degree of intercalation and higher tensile properties causes by formation of nanocomposites with better dispersion.

2. Experimental Section

2.1 Materials

A bacterial crystalline thermoplastic Polyhydroxybutyrate powder form was purchased from Sigma-Aldrich Chemic GmbH Company Germany. Polycaprolactone (CAPA 650) with number-average molecular weight of 50,000 was supplied by Solvay Caprolactone (England). Magnesium nitrate hexahydrate and aluminium nitrate nanohydrate were supplied by HmbG chemicals (Hamburg, Germany). Sodium hydroxide pellets was obtained from Merk (Darmstadt, Germany). Sodium stearate was purchased from R&M chemicals (Essex, UK).

2.2. Synthesis of Mg-Al LDH

The Mg-Al LDH was prepared via co-precipitation method. NaOH 1M solution was added drop by drop into a 250 ml solution of 19.22 g $Mg(NO_3)_2.6H_2O$ (0.2M) and 9.38 g $Al(NO_3)_3.9H_2O$ (0.067M) (with the mole ratio of 3:1 respectively) until pH 9 was acquired. It was carried out under vigorous stirring and constant flow of nitrogen, N_2 (g) to exclude carbon dioxide. The

resulting suspension was shaken and heated at 70°C in water bath shaker at 100 rpm of speed for about 16 hours. The slurry was filtered, washed methodically with distilled water and dried in oven at 60°C for 24 hours to obtain the Mg-Al LDH [32].

2.3. Preparation of stearate Mg-Al LDH

Preparation of stearate-Mg$_3$Al LDH via replacement of nitrate ions in the LDH layers with stearate ions from sodium stearate. One gram of the dry powder Mg-Al LDH was mixed with 1.8388 gram of sodium stearate and then dissolved in one liter distilled water. The mixture was stirred for 24 hours and aged at 70ºC of water bath to ensure complete reaction. Then, the white precipitate or slurry was filtered, washed with distilled water twice prior to drying at 60°C. The dried sample was ground and sieved into particles size of less than 100 micrometer.

2.4. Preparation of PHB/PCL Blends

PHB/PCL blends were prepared by solution casting method with different PCL contents (10, 20, 30, 40 and 50%). PHB and PCL were weighed, dissolution in 100 mL chloroform and stirred for one hour respectively. The two solutions were mixed and stirred for another 1 hour to obtain the homogeneous mixture solution. Besides, the mixture solutions were casted in a glass petri dish and dried in the solvent atmosphere to obtain sample films.

2.5. Preparation of PHB/PCL/stearate Mg-Al LDH Nanocomposites

From the characterization results of PHB/PCL blends, the optimum ratio of the blend was fixed at 80:20. The nanocomposites of PHB/PCL blend with different amount of stearate Mg-Al LDH (0.25, 0.5, 1, 1.5, 2%) were carried out by solution casting process. PHB, PCL and stearate Mg-Al LDH were dissolved and stirred in 100 mL chloroform for one hour respectively. Then mixed the three solutions together and stirred for another one hour. Solidification took place to evaporate excess amount of chloroform for 15 minutes. The mixture is poured on petri dish and left in fume cupboard for solvent evaporation to obtain dried films.

2.6 Characterization Methods and Instruments

2.6.1 Fourier Transform Infrared (FT-IR) Spectroscopy

The functional groups, types of bonding and identify components in the samples were determined by a Perkin Elmer Spectrum 1000 series Spectrophotometer equipped with attenuated total reflectance (ATR). The infrared spectra of the samples were recorded in the range of frequency of 400–4,000 cm^{-1}.

2.6.2 X-Ray Diffraction (XRD)

A Shimadzu XRD 6000 Diffractometer with nickel filtered Cu-Kα (λ = 0.1542 nm) beam operated at 30 kV and 30 mA was used to determine the interlayer d-spacing of the clay layer in the original Mg-Al LDH, modified stearate Mg-Al LDH, blends and nanocomposites using Bragg's equation $n\lambda = 2dsin\theta$. Data were recorded in 2θ range of 2º–30º using the scan rate of 2º/min.

2.6.3 Thermogravimetric Analysis (TGA)

Thermogravimetric Analysis (TGA) measures changes in the weight of a sample as a function of temperature and/or time. A Perkin-Elmer TGA Thermogravimetric Analysis was used in this study to define the maximum temperature and thermal stability of the LDH and intercalated samples. The samples were heated from 35ºC to 800°C at the rate of 10°C/min, nitrogen flow rate of 20ml/min and the weight that was used about 10-15 mg place in aluminium pan. The weight

and percentage of residue were recorded to determine the weight losses of the sample after heating.

2.6.4 Tensile Properties Measurement

Tensile test were carried out by a Universal Testing Machine, Instron 4302, according to ASTM D638-5. A crosshead speed of 5 mm/min and a load cell of 1 kN were used and the tests were performed at 25 ºC. The samples films were cut into dumb-bell shape using dumb-bell cutter (Die BS 6476) and thickness of the samples were measured using a thickness gauge. The results were expressed in term of tensile strength, tensile modulus and elongation at break. Seven specimens were tested and the averages of five best measurements were reported.

2.6.5 Scanning Electron Microscopy (SEM)

The scanning electron micrographs of tensile fracture surface of the samples were recorded by a JSM-6400 scanning microscope which is a state-of-the-art high resolution scanning electron microscope with a modern digital image processing system. This SEM Joel operated at 20 kV to investigate the surface morphology of samples. The samples were coated with gold by a Bio-rad coating system before viewing. The scanning electron micrographs were recorded at the magnification of 2000X.

2.6.6 Transmission Electron Microscopy (TEM)

The transmission electron micrographs of the thin layer of the nanocomposites were recorded by a LEO 912AB energy filter transmission electron microscope with an acceleration voltage of 100 keV. The thin layer of samples was prepared using a Reichert Jung Ultracut E microtome equipped with cryo-sectioning unit. The samples were sliced into thin layer of about 90 nm by a diamond knife cooled at –120 ºC with liquefied nitrogen.

3. Results and discussion

3.1 Characterization of Mg-Al LDH and stearate Mg-Al LDH

The Table 1, 2 and Fig. 1 shows the FT-IR spectra and peaks numbers of Mg-Al LDH and stearate Mg-Al LDH. An intense band which is shown in Mg-Al LDH at 1348.42 cm^{-1} is an asymmetric stretching vibration of nitrate anions [33]. From spectra 1(b) and 1(c) proved that the C−H stretching vibration due to the presence of the –CH$_3$ and –CH$_2$ groups of long chain stearate anions [34] are observed at 2800–3000 cm^{-1} which has no peak at the spectra 1(a).

Table 1. Characteristic infrared bands of Mg-Al LDH.

Band (cm^{-1})	Functional Groups
3399.51	O-H stretching
1642.30	H-OH stretching
1348.42	Asymmetric stretching vibration of nitrate anion
550.07	J-O and O-J-O (J = Mg or Al) lattice vibration

Meanwhile, two strong absorption peaks that located at 1566.73 cm^{-1} and 1455.02 cm^{-1} are assigned to carboxylate asymmetric and symmetric stretching [35]. As a conclusion, the stearate anions were successfully replacing the nitrate anions which intercalated between the layers.

Table 2. Characteristic infrared bands of stearate Mg-Al LDH.

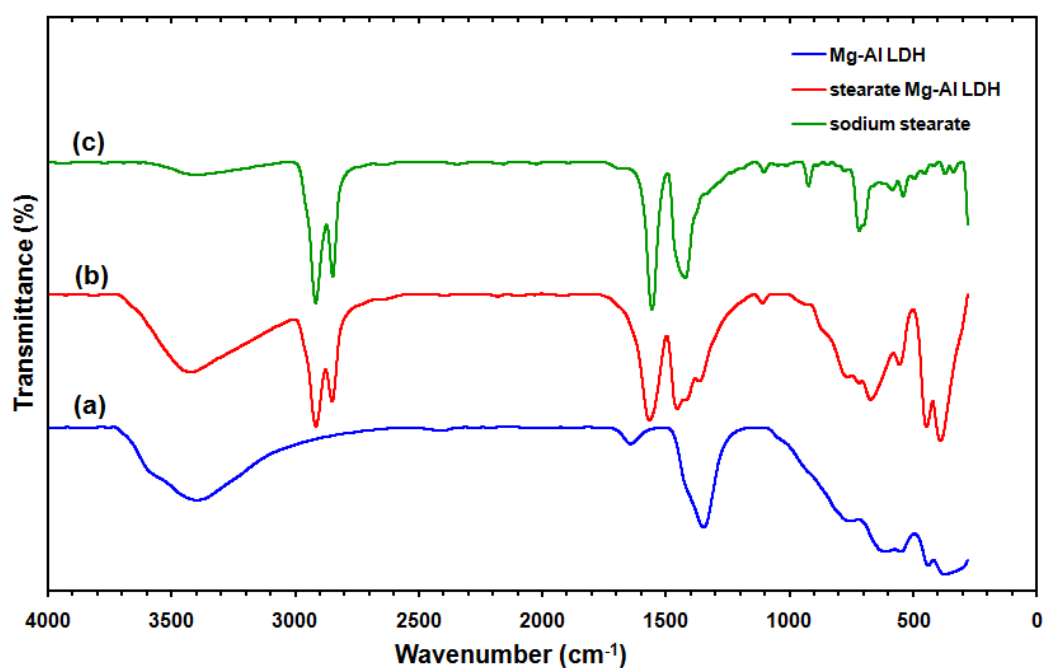| Band (cm⁻¹)	Functional Groups
3420.04	O-H stretching
2916.91	C-H stretching
2851.13	CH_2, CH_3 stretching
1566.73	Asymmetric carboxylate stretching
1455.02	Symmetric carboxylate stretching
558	M-O and O-M-O (M=Mg or Al) bonding

Fig. 1. FT-IR spectra for (a) pristine Mg-Al LDH, (b) stearate Mg-Al LDH and (c) sodium stearate.

The Table 3 and Fig. 2 shows the XRD patterns of Mg-Al LDH, stearate Mg-Al LDH and sodium stearate. The sodium stearate diffractogram shows a sharp peak at 2θ of 2.22º corresponding to the d-spacing of 39.80 Å proved that the organic modifier increasing clay interlayer distance. The chemical modification process indicating enhancement of d-spacing from 8.66 Å in Mg-Al LDH (corresponding 2θ value is 10.22°) to 32.97 Å in stearate Mg-Al LDH (corresponding 2θ value is 2.68°). This increment means that the long tail of hydrophobic chain of stearate anions increase the d-spacing by radiate away the hydrophobic side of stearate anion from surface and hydrophilic side reside in the interlayer of LDH [29].

Table 3. Interlayer spacing of different interlayer anion.

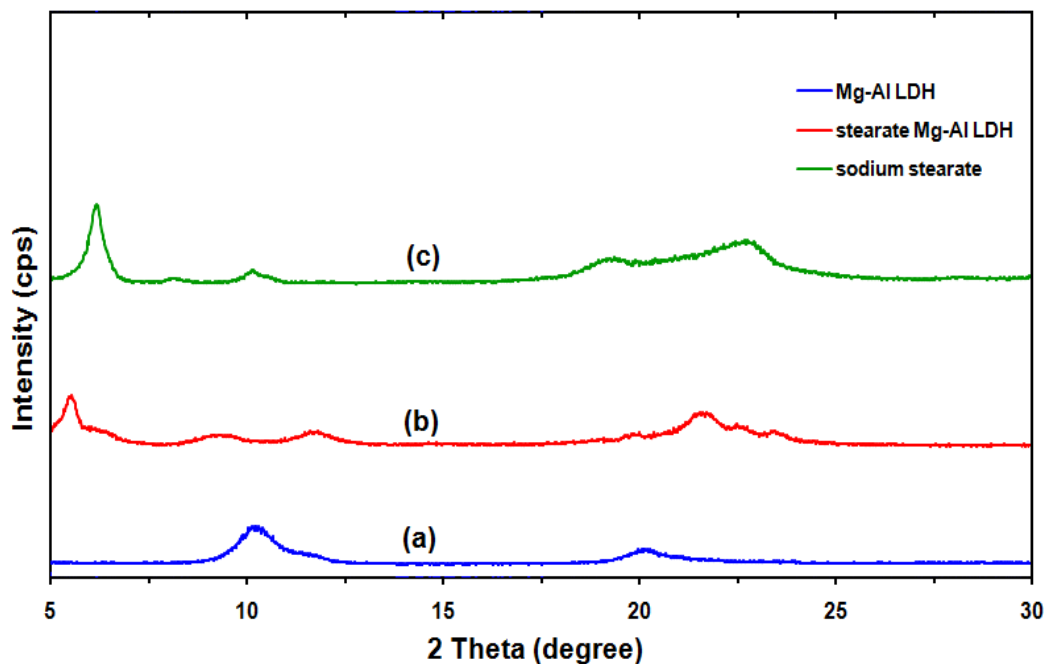| Type of clay	Exchange anions	Theta 2-Theta (Degree)	Interlayer spacing, d (Å)
Mg-Al LDH	NO_3^-	10.22	8.66
Stearate Mg-Al LDH	$H_3C(CH_2)_{16}COO^-$	2.68	32.97

Fig. 2. XRD patterns of (a) pristine Mg-Al LDH, (b) stearate Mg-Al LDH and (c) sodium stearate.

The Fig. 3 and Table 4 indicate the thermogram and derivative thermogram of both Mg-Al LDH and stearate Mg-Al LDH have two-stage of decomposition process. First stage decomposition is at around 150 °C where the interlayer water is desorbed. Loss of interlayer nitrate and dehydroxylation of the metal hydroxide layer occurs in second stage decomposition where complete collapse of the LDH structure at around 400 ºC. The maximum degradation temperature, T_{max} (ºC) of Mg-Al LDH and stearate Mg-Al LDH is 425.67 ºC and 385.12 ºC respectively.

The improvement of onset temperature in the Mg-Al LDH is corresponds to the inorganic nitrate which are more thermally stable than the organic stearete anions in stearate Mg-Al LDH. Besides, reaction in the interlayer Mg-Al LDH with the interaction of strong hydrogen bonds between interlayer water molecules, nitrate anions and hydroxide sheets. Moreover, the present of organic compound sodium stearate exhibit more easily degraded than Mg-Al LDH. Therefore, it has higher maximum degradation temperature compare to stearate Mg-Al LDH.
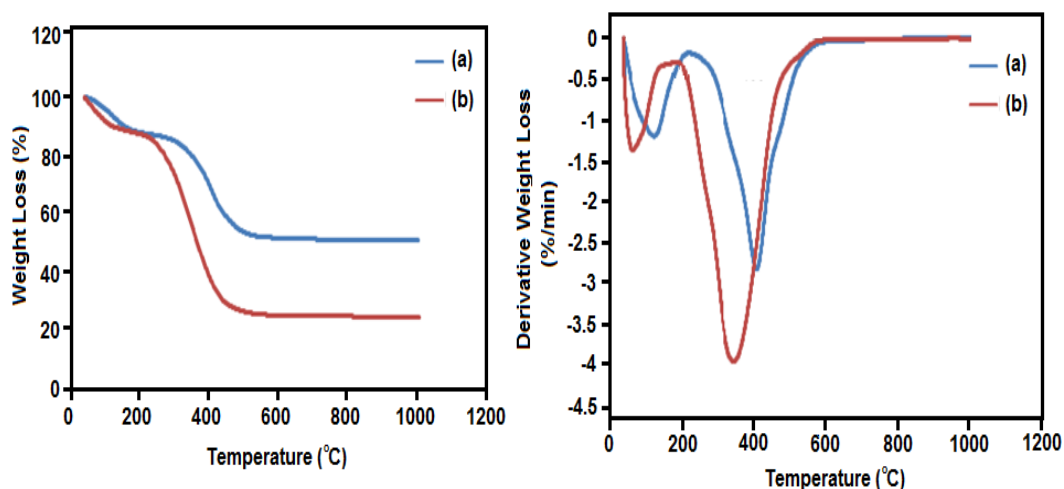

Fig. 3. TGA analysis and DTG thermograms for Mg-Al LDH and stearate Mg-Al LDH.

Table 4. Summary of onset temperature, maximum degradation temperature and percentage of weight loss for Mg-Al LDH and stearate Mg-Al LDH.

Type of LDH	Weight loss at T_1 (%)	Weight loss at T_2 (%)	Onset temperature at T_1 (°C)	Onset temperature at T_2 (°C)	Maximum degradation temperature T_{max} (°C)
Mg-Al LDH	10.816	35.176	178.11	220.47	425.67
Stearate Mg-Al LDH	13.231	63.932	145.05	208.55	385.12

3.2 Characterization of PHB/PCL/stearate Mg-Al LDH Nanocomposites

The different content of stearate Mg-Al LDH was added with 80PHB/20PCL blend to formed PHB/PCL/stearate Mg-Al LDH nanocomposites. 80PHB/20PCL blend was chosen as our optimum blend because of application such as plastics and packaging field were focused on the tensile strength and elongation at break. Meanwhile, this blend weight ratio gives the higher value of mechanical properties. Figure 4 and Table 5 shows the almost same FT-IR spectra of pure PHB, pure PCL, 80PHB/20PCL blend and PHB/PCL/stearate Mg-Al LDH nanocomposites with different stearate Mg-Al LDH content. The similar functional group of both polymer resulting no any major peak shifting or formation of new peak in the blend and nanocomposites spectra caused by no strong chemical interaction and bonding between PHB, PCL and stearate Mg-Al LDH [36].
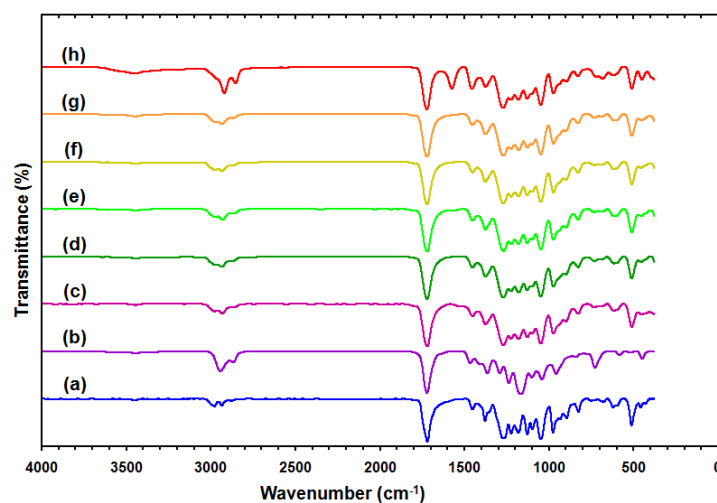

Fig. 4. FT-IR spectra of (a) pure PHB, (b) pure PCL, (c) 80PHB/20PCL blend and PHB/PCL/stearate Mg-Al LDH nanocomposite with (d) 0.25, (e) 0.5, (f) 1, (g) 1.5 and (h) 2 wt% stearate Mg-Al LDH content.

Table 5. Characteristic infrared bands of PHB/PCL/stearate Mg-Al LDH nanocomposites.

Band (cm^{-1})	Functional Groups
3400	O-H stretching
2800-3000	C-H stretching
1700	C=O stretching vibration
1400	C-H bending vibration in CH$_3$ group
1300	C-O-H bonding
1100	C-O stretching

The Fig. 5 shows the XRD patterns of pure PHB, pure PCL, optimum ratio of PHB/PCL blend and PHB/PCL/LDH nanocomposites of various amounts of the stearate Mg-Al LDH

contents. The absence of the main diffraction peak at around 2.00° for very low concentration such as 0.25 and 0.5 wt% stearate Mg-Al LDH nanocomposites shows that the LDH layers are completely exfoliated and randomly dispersed in the PHB/PCL polymer blend matrix [32]. For the nanocomposites that containing 1, 1.5 and 2 wt% stearate-Mg_3Al LDH nanocomposites there is a very small peak at 2θ of 2.195°, 2.275° and 2.325° with 40.20 Å, 38.78 Å and 38.00 Å interlayer spacing respectively. This increment of d-spacing indicating that polymer chains are intercalated into the clay layers to form intercalated type nanocomposites.
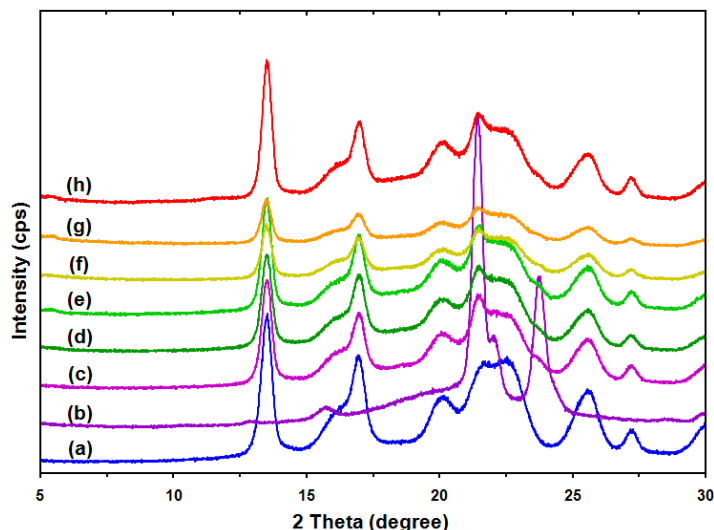

Fig. 5. XRD patterns of (a) pure PHB, (b) pure PCL, (c) 80PHB/20PCL and PHB/PCL/stearate Mg-Al LDH nanocomposites with (d) 0.25, (e) 0.5, (f) 1, (g) 1.5 and (h) 2 wt% stearate Mg-Al LDH content.

In the Fig. 6 shows the TG and DTG curves for the thermal degradation of PHB/PCL nanocomposites. More exfoliated particles were observed when increasing the filler content, resulting an improvement thermal stability of the nanocomposites until the critical value which was addition 1.0 wt% stearate Mg-Al LDH. This proved by the lower weight loss 85.32% and higher maximum degradation temperature 329.59 ºC. Moreover, higher thermal stability indicating that there is well homogeneous mixing or strong hydrogen bond interaction between the hydroxyl groups of the clay layers and carbonyl groups of polymer matrix. With the further increasing stearate Mg-Al LDH loading resulting decrease in thermal stability because of the complete exfoliation will restricted or interrupted due to geometrical restraints within the inadequate space available in the polymer matrix and formation of agglomeration.
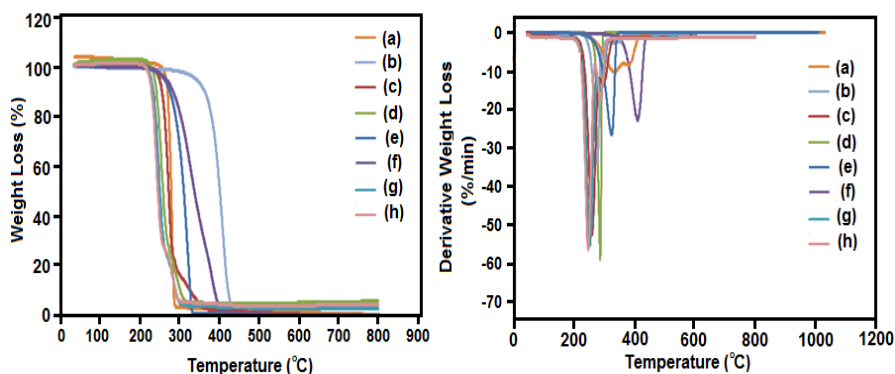

Fig. 6. TGA analysis and DTG thermograms for (a) pure PHB, (b) pure PCL, (c) 80PHB/20PCL and PHB/PCL/stearate Mg-Al LDH nanocomposites with (d) 0.25, (e) 0.5, (f) 1, (g) 1.5 and (h) 2 wt% stearate Mg-Al LDH content.

The formation of nanocomposites can be directly observed by TEM. The transmission electron micrographs of optimum 80PHB/20PCL polymer blend and 80PHB/20PCL/1stearate Mg-Al LDH nanocomposites are shown in Fig. 7 In the Fig. 7 (a), same polarities of both polymers are dispersed well together. Additional of 1.0 wt % stearate Mg-Al LDH clay, the dark lines in Fig. 7 (b) represent the LDH layers in the PHB/PCL polymer matrix with the formation of mixture of intercalated and exfoliated type nanocomposites.
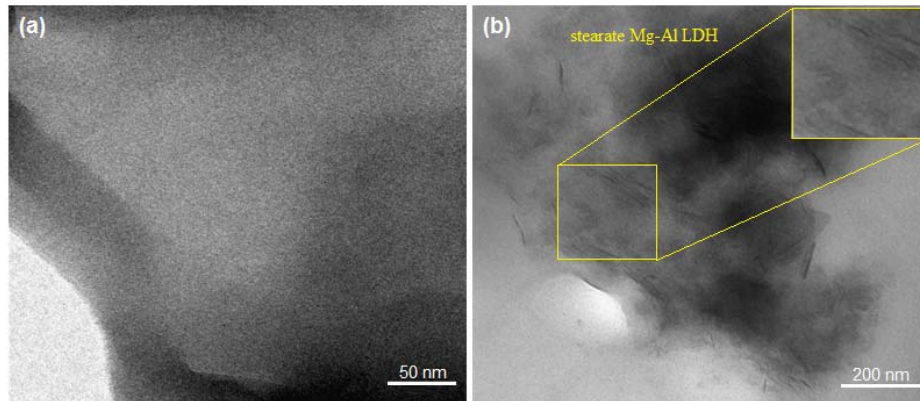

Fig. 7. Transmission electron micrographs of (a) 80PHB/20PCL blend and (b) 80PHB/20PCL/1wt% stearate Mg-Al LDH nanocomposites.

The Fig. 8 shows the tensile strength, modulus and elongation at break of PHB/PCL/stearate Mg-Al LDH nanocomposites with effect of different stearate Mg-Al LDH content. The tensile strength of neat PHB is 23.00 MPa and decrease to 17.02 MPa upon the addition of 20PCL. However, addition of 1.0 wt% of stearate Mg-Al LDH into 80PHB/20PCL blend increasing the tensile strength to 28.23 MPa or an enhancement of 66% compared to the unfilled clay PHB/PCL blends.
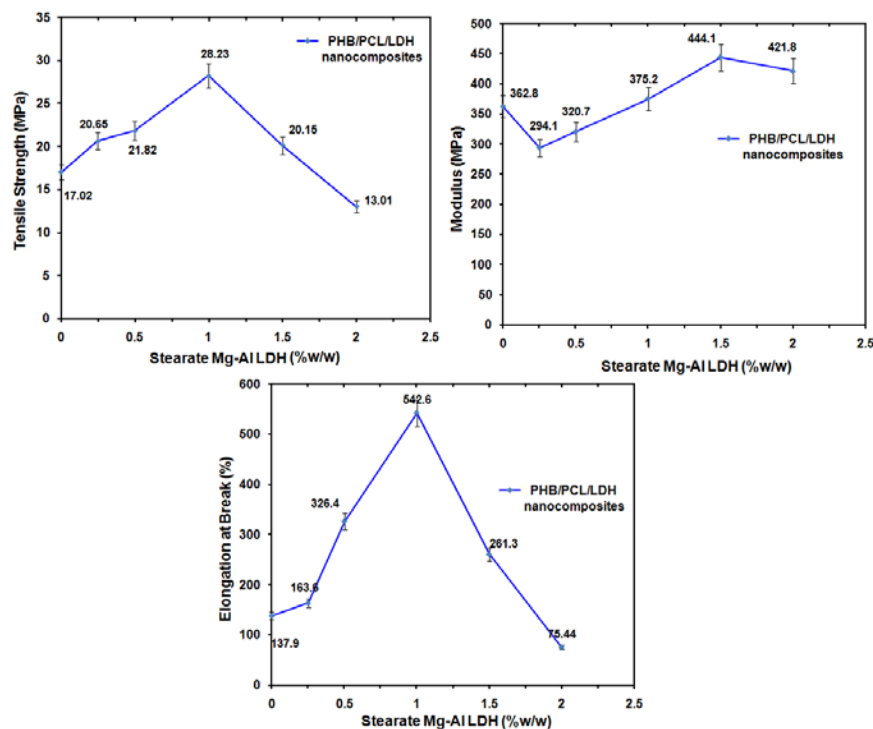

Fig. 8. Tensile strength, Modulus and Elongation at break of PHB/PCL/stearate Mg-Al LDH nanocomposites with 0.25, 0.5, 1, 1.5 and 2 wt% stearate Mg-Al LDH content.

This is causes by the strong interfacial adhesion between the polymer matrix and filler. Further addition of high filler content probably favours the formation of inorganic clusters or agglomerates, therefore reduces the tensile strength. The tensile modulus of PHB/PCL/stearate Mg-Al LDH nanocomposites increases with the increase of stearate Mg-Al LDH content which higher content of filler will lead to restriction of the polymer chains from the interaction with the clay surface [37].

Nanocomposites with 1.0 wt% stearate Mg-Al LDH produced higher improvement in elongation at break which is 300% higher as compared with that 80PHB/20PCL blend. Stearate anions consider as plasticizer since their long hydrocarbon segments improve the flexibility of polymer matrix [38]. However, further addition of stearate Mg-Al LDH decrease the elongation at break due to extended agglomerates which makes the nanocomposites to be more brittle [39, 40].

In the Fig. 9 shows SEM micrographs obtained from the tensile fracture surfaces of PHB/PCL blend and its nanocomposites containing 0.25, 0.5, 1, 1.5 and 2 wt% of stearate Mg-Al LDH. Image 9 (a) shows the fractured surface of optimum PHB/PCL blend with rough surface which reduce the rigidity of the samples. The Fig. 9 (b-e) shows rough and well stretched surface before it breaks, indicating the presence of the stearate Mg-Al LDH improves the compatibility and flexibility in nanocomposites [36]. This reveals that stearate Mg-Al LDH is a good compatibilizer that enhances the miscibility and interaction between the polymer matrix and filler.
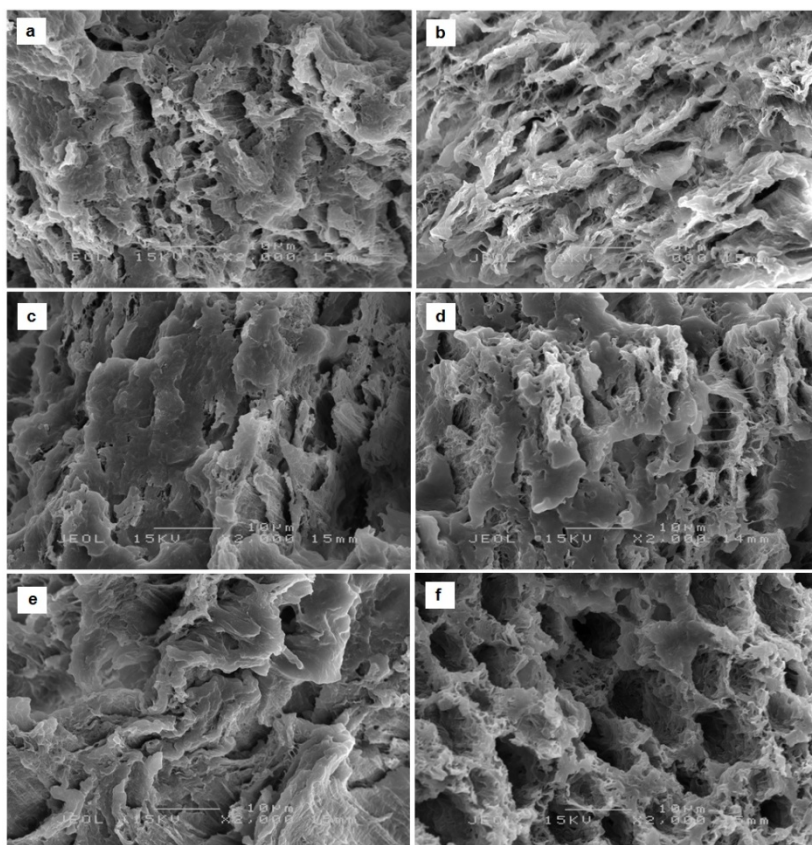

Fig. 9. Scanning electron mircographs of (a) 80PHB/20PCL blend and PHB/PCL/stearate Mg-Al LDH nanocomposites with (b) 0.25, (c) 0.5, (d)1, (e) 1.5 and (f) 2 wt% stearate Mg-Al LDH content at 2000x magnification.

4. Conclusion

Modification of stearate Mg-Al LDH was successfully prepared by chemical modification via ion exchange reaction. Besides, PHB/PCL/stearate Mg-Al LDH nanocomposites were prepared via through solution casting method by used of chloroform as organic solvent. There is no major peak shifting and no formation of new peak in FT-IR spectrum indicated no strong interaction

among PHB, PCL and stearate Mg-Al LDH. Besides, XRD analysis reveals that presence of 1.0 wt% of stearate Mg-Al LDH content show higher interlayer spacing and more easier polymer chain intercalated into interlayer LDHs. TEM result proven that the homogeneous dispersion of 1.0 wt % stearate Mg-Al LDH lead to strong interaction adhesion between polymer matrix and filler which resulting in the higher thermal stability. Mechanical analyses showed that an 80PHB/20PCL/1stearate Mg-Al LDH nanocomposite was drastically enhanced about 66% and 300% its tensile strength and elongation at break. These improvements have been exhibited by SEM where the incorporation of stearate Mg-Al LDH clay gradually increases the flexibility and compatibility of nanocomposites.

Acknowledgment

References

[1]. M.D. Sanchez-Garcia, E. Gimenez, J.M. Lagaron. Carbohydr. Polym. **71**(2), 235 (2008).
[2]. D.Z. Bucci, L.B.B. Tavares, I. Sell. Polym. Test. **24**, 564 (2005).
[3]. Y.S. Chun, J. Park, J.B. Sun, W.N. Kim. J. Appl. Polym. Sci: Part B: Polyme Phy. **38**(15), 2072 (2000).
[4]. C. Hinüber, L. Häussler, R. Vogel, H. Brünig, G. Heinrich, C. Werner. Express Polym. Lett. **5**(7), 643 (2011).
[5]. M.B. Ahmad, K. Shameli, W.M.Z. Wan Yunus, N.A. Ibrahim, Aust. J. Basic. Appl. Sci. **4** (7), 2158 (2010).
[6]. M.B. Ahmad, K. Shameli, W.M.Z. Wan Yunus, N.A. Ibrahim. Am. J. Appl. Sci. **6** (11), 1909 (2009).
[7]. M.B. Ahmad, M.Y. Tay, K. Shameli, M.Z. Hussein, J.J. Lim. Int. J. Mol. Sci. 12 (8), 4872 (2011).
[8]. K. Shameli, M.B. Ahmad, S.D. Jazayeri, P. Shabanzadeh, P. Sangpour, H. Jahangirian, Y. Gharayebi. Chem. Cent. J. **6** (1), 1 (2012).
[9]. K. Shameli, M.B. Ahmad, Jaffar E.A. Al-Mulla, N.A. Ibrahim, P. Shabanzadeh, A. Rustaiyan, Y. Abdollahi, S. Bagheri, M. Sani Usman, M. Zidan. Molecules **17** (7), 8506 (2012).
[10]. K. Shameli, M.B. Ahmad, E.A.J. Al-Mulla, N.A. Ibrahim, P. Shabanzadeh, A. Rustaiyan, Y. Abdollahi, S. Bagheri, S. Abdolmohammadi, M.S. Usman, M. Zidan. Molecules **17** (7), 8506 (2012).
[11]. M.B. Ahmad, J.J. Lim, K. Shameli, N.A. Ibrahim, M.Y. Tay. Molecules **16** (9), 7237 (2011).
[12]. K. Shameli, M.B. Ahmad, S.D. Jazayeri, P. Shabanzadeh, H. Jahangirian, M. Mahdavi, Abdullahi, Y. Int. J. Mol. Sci. **13** (6), 6639 (2012).
[13]. K. Shameli, M.B. Ahmad, A. Zamanian, P. Sangpour, P. Shabanzadeh, Y. Abdollahi, M. Zargar. Int. J. Nanomed. **7**, 5603 (2012).
[14]. M.B. Ahmad, K. Shameli, W.M.W. Wan Yunus, N.A. Ibrahim, A.A. Hamid, M. Zargar. Res. J. Biol. Sci. **4** (11), 1156 (2009).
[15]. M.B. Ahmad, J.J. Lim, K. Shameli, N.A. Ibrahim, M.Y. Tay, B.W. Chieng. Chem. Cent. J. **6** (1), 1 (2012).
[16]. K. Shameli, M.B. Ahmad, W.M.W. Wan Yunus, N.A. Ibrahim, M. Jokar. Proc. World Acad. Sci., Eng. Technol. 64, 28 (2011).
[17]. P. Shabanzadeh, N. Senu, K. Shameli, F. Ismail, Dig. J. Nanomater. Bios. **8**(3), 1133 (2013)
[18]. P. Shabanzadeh, N. Senu, K. Shameli, M. Mohaghegh Tabar, E-J. Chem. 1–8 (2013)
[19]. P. Shabanzadeh, N. Senu, K. Shameli, F. Ismail, M. Mohaghegh Tabar, Dig. J. Nanomater. Bios. **8**(2), 541 (2013)
[20]. P. Shabanzadeh, N. Senu, K. Shameli, F. Ismail, A. Zamanian, M. Mohaghegh Tabar. Res. Chem. Intermed. 1-13 (2013).
[21]. S.R. Lee, H.M. Park, H. Lim, T. Kang, X. Li, W.J. Cho, C.S. Ha. Polymer **43**, 2495 (2002).

[22]. Y. Kameshima, H. Yoshizaki, A. Nakajima, K. Okada. J. Colloid Interface Sci. **298**(2), 624 (2006).

[23]. Y.Q. Shi, F. Chen, J.T. Yang, M.Q. Zhong, Appl. Clay. Sci. **50**, 87 (2010).

[24]. H.M. Park, W.K. Lee, C.Y. Park, W.J. Cho, C.S. Ha. J. Mater Sci. **38**, 909 (2003).

[25]. S. Pradhan, F.R. Costa, U. Wagenknecht, D. Jehnichen, A.K. Bhowmick, G. Heinrich. Eur. Polym. J. **44**, 3122 (2008).

[26]. C. Manzi-Nshuti, P. Songtipya, E. Manias, M.M. Jimenez-Gasco, J. M. Hossenlopp, C.A. Wilkie. Polymer **50**, 3564 (2009).

[27]. F.R. Costa, A. Leuteritz, U. Wagenknecht, D. Jehnichen, L. Häußler, G. Heinrich. Appl. Clay. Sci. **38**, 153 (2008).

[28]. M.D. Sanchez-Garcia, E. Gimenez, J.M. Lagaron. J. Appl. Polym. Sci. **108**(5), 2787 (2008).

[29]. L. Sang-Rock, P. Hwan-Man, L. Hyuntaek, K. Taekyu, L. Xiucuo, C. Won-Jei. Polymer **43** 2495 (2002).

[30. M. Eili, K. Shameli, N.A. Ibrahim, W.M.Z. Wan Yunus. Int. J. Mol. Sci. **13**, 7938 (2012).

[31. Y. Ding, Z. Gui, J. Zhu, Y. Hu, Z. Wang. Mater. Res. Bull. **43**, 3212 (2008).

[32]. J. Liu, G. Chen, J. Yang. Polymer **49**, 3923 (2008).

[33]. H.B. Hsueh, C.Y. Chen. Polymer **44**, 1151 (2003).

[34]. J. Sharif, W.M.Z. Wan Yunus, Z.H.M.D. Khairul, B.A. Mansor. Polym. Test. **24**, 211 (2005).

[35]. H. Essawy, D. El-Nashar. Polym. Test. **23**, 803 (2004).

[36]. J.S. Shelley, P.T. Mather, K.L. DeVries, Polymer **42**(13), 5849 (2001).

[37]. Pozsgay, A., Frater, T., Szazdi, L., Muller, P., Sajo, I., Pukanszky, B. 2004. Eur. Polym. J. **40**, 27–36.

[38]. Cao, N., Yang, X., Fu, Y. Food Hydrocolloid **23**, 729 (2009).

[39]. N. Hasegawa, M. Kawasumi, M. Kato, A. Usuki, A. Okada, J. Appl. Polym. Sci. **67**, 87 (1998).

[40]. L. Averous, L. Moro, P. Dole, C. Fringant. Polymer. **41,** 4157 (2000).